ACS Chemical Neuroscience

Research Article

pubs.acs.org/acschemicalneuroscience

Potential of a γ-Glutamyl-Transpeptidase-Stable Glutathione Analogue against Amyloid-β Toxicity

Swati S. More and Robert Vince*

Center for Drug Design, Academic Health Center, University of Minnesota, Minneapolis, Minnesota 55455, United States

Supporting Information

ABSTRACT: The antioxidant properties of glutathione (GSH) and their relevance to oxidative stress induced pathological states such as Alzheimer's disease is well-established. The utility of GSH itself as a pharmacotherapeutic agent for such disorders is limited because of the former's lability to breakdown through amide cleavage by the ubiquitous enzyme γ-glutamyl transpeptidase (γ-GT). In the present study, a GSH analogue, Ψ-GSH, where the γ-glutamylcysteine amide linkage is replaced with a ureide linkage, was synthesized. Ψ-GSH was found to be stable toward γ-GT mediated breakdown. Ψ-GSH fulfilled four cardinal properties of GSH, namely, traversing across the blood brain barrier (BBB) via the GSH active uptake machinery, replacing GSH in the glyoxalase-I mediated detoxification of methylglyoxal, protecting cells against chemical oxidative insult, and finally lowering the cytotoxicity of amyloid-β peptide. These results validate Ψ-GSH as a viable metabolically stable replacement for GSH and establish it as a potential preclinical candidate for treatment of oxidative stress mediated pathology.

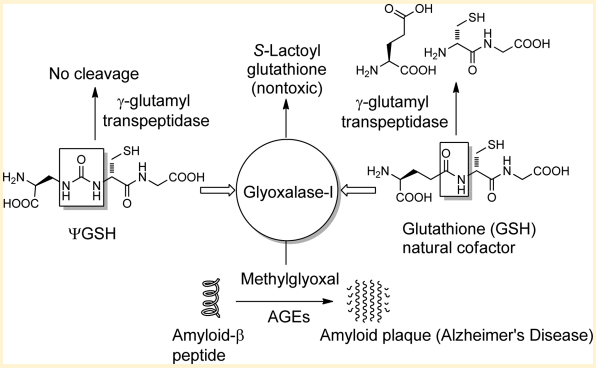

KEYWORDS: *Glutathione, glyoxalase I, Alzheimer's disease, β-amyloid peptide, methylglyoxal, advanced glycation end products*

Alzheimer's disease (AD) is the seventh leading cause of death in the United States. With 5.3 million people currently suffering from the disease, the total expenditure on treatment is as high as 172 billion dollars per year.[1] Exceptions aside, AD is a disease of aging whose causative factors are incompletely delineated; nevertheless, its pathology is well-defined. In the absence of other disease states, adult onset dementia is an empirical indicator of AD. Prominent microscopic markers are extracellular senile plaques (SP, amyloidosis) and intracellular neurofibrillary tangles (NFTs).[2] Both of these neuropathologies are shown to negatively affect synaptic function.[3] The AD-afflicted brain shows markedly high indicators of oxidative stress, an umbrella term that describes concentration of species causing oxidative protein, lipid, and DNA modification. Examples of such stressors are Fe^{2+}, which can abstract an electron from dioxygen to form reactive oxygen species (ROS) such as the superoxide radical ($O_2^{\bullet}$) and hydrogen peroxide as well as dicarbonyl species such as methylglyoxal (MG) and glyoxal.[4] Condensation of glucose and dicarbonyl compounds with amino groups of proteins is also an oxidative stressor, as the Schiff bases can then rearrange and/or react further to form irreversibly modified proteins (advanced glycosylation end products, AGEs).[5]

SPs are aggregates of the 42-amino acid amyloid-β peptide (Aβ), derived in turn from the amyloid precurssor protein (APP), a structural and functional component of synapses. β- and γ-Secretases cleave APP into Aβ, which is in turn metabolized by a range of zinc metalloproteinases. Products of APP cleavage, including Aβ, participate in regulation of excitatory neurotransmission and may fulfill other hitherto unknown electrophysiological roles.[6,7] While production of Aβ is a normal physiological event, conformational changes in Aβ that lead to its aggregation have no known physiological roles. Among the three interchanging solution conformations of Aβ, namely, a random coil, an α-helix, or a β-sheet, the latter possesses a dramatically higher tendency to aggregate. Aβ in an antiparallel β-sheet conformation nucleates fibrillogenesis, with other monomers assuming similar conformation to result initially in soluble aggregates. Higher order aggregation eventually forms fibrils and progressively renders the growing aggregate insoluble. Nucleation is shown to be rate-limiting for Aβ aggregation.[8] MG-modified Aβ peptides known to more potently nucleate aggregate formation than the unmodified peptides.[9] AGEs upregulate APP expression through increase in ROS concentrations, adding to their propensity to cause Aβ aggregate formation.[10] NFTs consist of stable aggregated bifilar helices (paired helical fragments, PHF) derived from the microtubule stabilizing τ-proteins.[11] Phosphorylation and covalent (AGE) modification of the lysine residues in the tubulin-binding motif of τ-proteins promote its detachment from tubulin and subsequent aggregation.[12,13] Aβ fibrils are known to induce τ-phosphorylation and decrease microtubule

Received: November 15, 2011
Accepted: January 3, 2012
Published: January 3, 2012

binding of τ-proteins, thereby promoting NFT formation.[14] ROS thus influence the formation of both of these abnormal protein aggregates.

Glutathione (GSH) is the primary thiol reductant utilized by physiological pathways that counteract ROS. GSH levels are dynamically maintained through its consumption by detoxifying enzymes, for example, glutathione peroxidase (GSHPx) and by metabolic enzymes, for example, γ-glutamyl transpeptidase (γ-GT), its de novo synthesis involving glutamate cysteine ligase (GCL), glutathione synthetase (GSS), and regeneration mediated by glutathione reductase (GR). Aging tissue shows upregulation of GSHPx, Glx-I, and GR, but reduced GCL activity either through downregulation of expression or through impairment of the enzyme's catalytic subunit.[15,16] GSH levels are invariably depleted in aging and AD-afflicted brain.[17,18] Whether GSH depletion is secondary to AD development or is a contributory factor is indeterminate, nevertheless, elevation of GSH levels as a means to counteract the oxidative damage in AD is a well-supported hypothesis.[19] Unfortunately, direct oral GSH administration does not result in significant systemic elevation of GSH levels because of intestinal and hepatic γ-GT.[20]

The present study aims to evaluate a glutathione surrogate (Ψ-GSH; Figure 1) that could potentially substitute for GSH

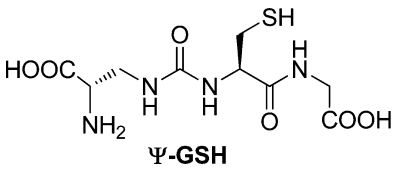

Figure 1. Structure of Ψ-GSH.

while possessing resistance to γ-GT mediated metabolism. It is expected that Ψ-GSH would be resistant to γ-GT by virtue of the substitution of the γ-glutamyl-cysteine amide with a urea isostere. A γ-GT-resistant glutathione analogue would in turn be expected to possess longer residence time in the cell, conferring upon the analogue improved apparent potency over GSH for antioxidant activity. Successful substitution of GSH would entail fulfillment of principal GSH abilities and functions. In this study, we regarded the following properties of GSH as necessary prerequisites for a viable GSH replacement: (1) BBB penetration via recognition by the active transport machinery for GSH; (2) ability to function as a GSH surrogate for the Glx-I mediated detoxification of MG into lactate (3) ability to protect cells against direct oxidative insults (e.g., H_2O_2 and MG), and finally (4) ability to protect cells against exposure to Aβ.

RESULTS AND DISCUSSION

Ψ-GSH was synthesized from the previously reported protected peptide **1**.[21] The *t*-butyl carbamate and *t*-butyl ester protecting groups were removed concomitantly in TFA, followed by reductive removal of the S−S*t*Bu protecting group (Scheme 1). Ψ-GSH obtained after chromatography over C-18 bonded silica gel was found to be 96% pure by HPLC and its structure was intact according to ^{1}H and ^{13}C NMR spectra.

No appreciable degradation of Ψ-GSH was observed during its incubation with γ-GT for up to 24 h, while GSH was completely degraded by γ-GT within 30 min (Supporting Information; Figure S1). This was in accordance with our

Scheme 1. Synthesis of Ψ-GSH

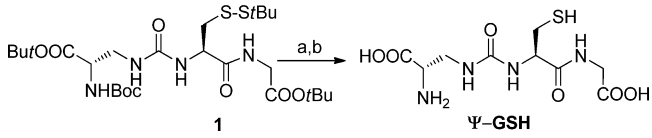

observations with the properties of similar previously reported analogues and derivatives of Ψ-GSH.[21,22] Formation of the γ-glutamyl cysteine amide bond is a rate-limiting step in the synthesis of GSH, a fact that compounds the GCL deficiency in aging and Alzheimer's disease afflicted tissue.[15] Provision of a γ-glutamyl cysteine motif in such cases would address that crucial deficiency. In fact, supplementation with γ-glutamyl cysteine has been found to yield an antioxidant effect and increase GSH levels.[23] However, such a dipeptide does not address the problem of continual γ-GT mediated GSH metabolism. Ψ-GSH is rendered immune to such a drawback due to demonstrated resilience to γ-GT.

Glx-I was found to recognize Ψ-GSH and mediate its addition to MG to form hemimercaptal **2** (Scheme 2). The

Scheme 2. Glx-I Mediated Formation of 2

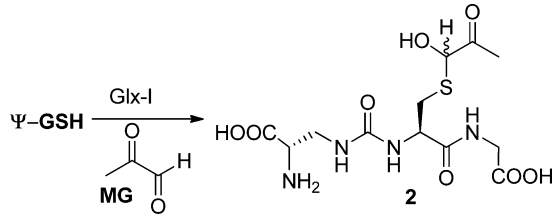

slopes for initial velocity vs substrate concentration were 0.0498 ± 0.0040 for Ψ-GSH and 0.1954 ± 0.0216 for GSH (Figure 2).

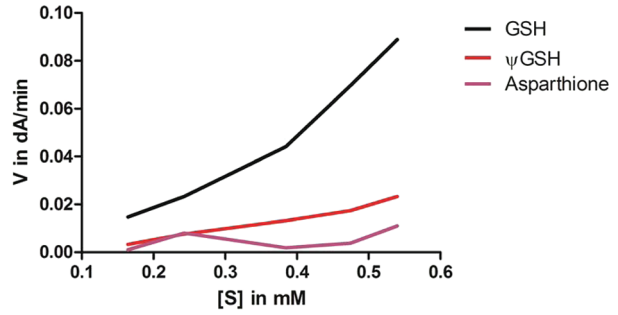

	GSH	ψGSH	Asparthione
Slope	0.195 ± 0.022	0.050 ± 0.004	0.013 ± 0.014

Figure 2. Glyoxalase I enzyme kinetics assay. GSH or ΨGSH at various concentrations was incubated with MG at 30 °C in phosphate buffer (0.05 M, pH 6.6) for 6 min to allow formation of the hemimercaptal **2**, followed by the addition of yeast Glx-I. The enzyme reaction was monitored for 180 s by measuring the increase in absorption at 240 nm. Rates of enzymatic reaction were plotted against substrate concentrations. Data shown here is representative of three independent experiments.

In comparison, the corresponding slope the best known alternative cofactor for the Glx-I reaction, asparthione, had a value of 0.0132 ± 0.0136.[24] Ψ-GSH is thus not just a viable

dx.doi.org/10.1021/cn200113z | ACS Chem. Neurosci. 2012, 3, 204−210

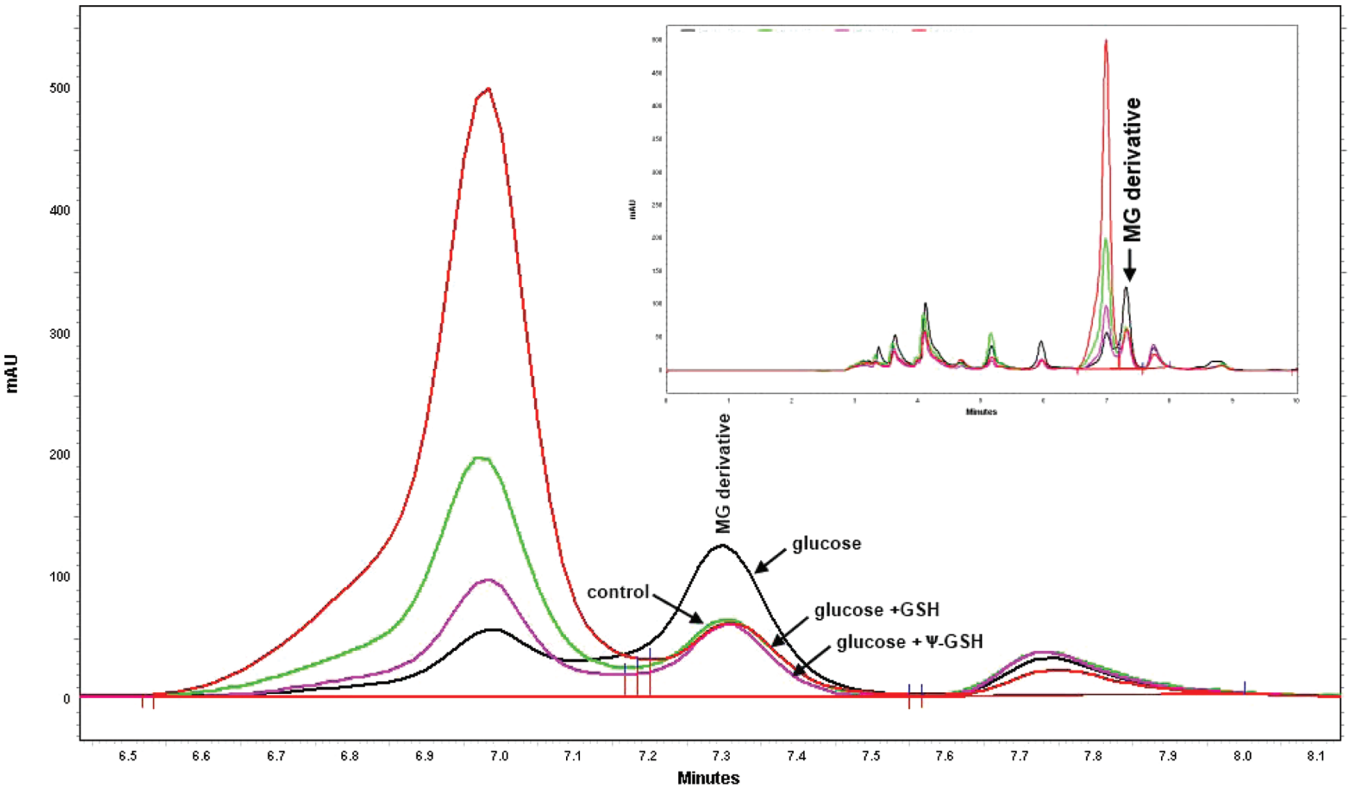

Figure 3. Effect of GSH and Ψ-GSH on intracellular levels of methylglyoxal. SH-SY-5Y cells were treated with glucose (50 mM) for 72 h in the presence and absence of GSH or Ψ-GSH (500 μM). Intracellular concentrations of MG were quantified by HPLC after derivatization with 1,2-diaminobenzene as described in Methods. The results of this experiment demonstrated that GSH and Ψ-GSH caused reduction in MG levels to similar extents.

substrate for the Glx-I detoxification pathway; it is a better substrate than any other known alternative substrates. Its relatively slower rate of reaction when compared to GSH would be well-compensated by increased residence time of Ψ-GSH.

MG-scavenging activity of Ψ-GSH was next examined in a cell-based assay. A 2.1-fold increase in the production of MG in SH-SY-5Y cells over untreated controls could be induced by incubation with 50 mM glucose for 3 days (Figure 3). Preincubation of these cells with either GSH or Ψ-GSH before glucose exposure prevented glucose-induced intracellular MG accumulation. Importantly, Ψ-GSH inhibited MG accumulation to an extent comparable to that of GSH, perhaps stemming from its higher stability despite being a poorer substrate than GSH. Hyperglycemia-induced intracellular MG accumulation has shown to be involved in diabetes-related cellular damage; this is an area where Glx-I substrates such as Ψ-GSH could prove futile apart from its potential application in Alzheimer's disease.[25]

Aβ elicits its cytotoxicity at least in part through its ability to provoke intracellular ROS formation, as it has been shown that antioxidants can prevent Aβ-induced cell death in vitro.[26] Treatment of SH-SY-5Y cells with 20 μM Aβ (1-42) caused significant (48.2%) loss of cell viability, evidenced through decrease in cell number and mitochondrial activity (Figure 4A). Pretreatment of the cells with GSH or Ψ-GSH for 24 h caused dose-dependent resistance to Aβ toxicity. Concentrations of 10 μM of both compounds fully protected the cells, with the protection obtained with Ψ-GSH being significantly higher statistically ($p < 0.05$) than that with GSH. Of particular note is the length of Ψ-GSH-induced cytoprotection that was 5 days, as opposed to that with GSH, which was significant only until

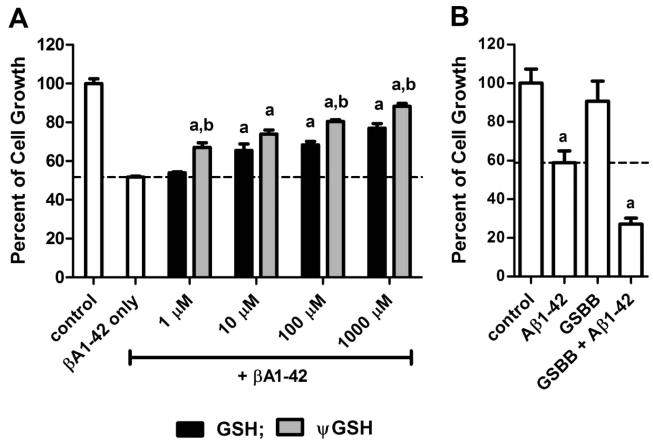

Figure 4. Protection against Aβ1-42 cytotoxicity by GSH and Ψ-GSH. The percent cell death caused in SH-SY-5Y cells by 24 h exposure to Aβ1-42 (20 μM) exposure was determined by the standard MTT assay as described in Methods. The decrease in cytotoxicity of Aβ1-42 was observed by preincubation of cells with (A) GSH or ΨGSH and (B) GSBB (1 mM) for 24 h and was dose-dependent with respect to their concentrations. Data are expressed as the (mean ± SEM) of three independent experiments (a, significantly higher than βA1−42 only group, $p < 0.0001$; b, significantly higher than corresponding GSH treatment group, $p < 0.05$).

day 3 (Supporting Information; Figure S2). The higher duration of protection conferred by Ψ-GSH could be due to its higher stability to γ-GSH mediated metabolism.

The mechanism of Aβ-induced cell damage may encompass any number and types of ROS. The significance of MG in the

dx.doi.org/10.1021/cn200113z | ACS Chem. Neurosci. 2012, 3, 204−210

toxicity induced by Aβ was evaluated by preventing intracellular detoxification of MG through inhibition of Glx-I with an inhibitor, *S*-*p*-bromobenzylglutathione (GSBB).[27] Incubation of SH-SY-5Y cells with 1 mM GSBB caused 10% cell death. Percentage cell viability after treatment with Aβ alone and in combination with GSBB was 58.95 and 23.60, respectively (Figure 4B; $p < 0.0001$). It therefore appears that MG is an important ROS generator in Aβ induced cell damage.

One of the pathways through which Aβ causes intracellular ROS accumulation is through production of H_2O_2 in the presence of Cu(II).[28] Damage caused by H_2O_2 contributes to the loss of synaptic function.[29,30] GSH can directly neutralize H_2O_2 either through chemical reduction or by functioning as the sacrificial reductant in the GSHPx mediated reduction of H_2O_2. The ability of Ψ-GSH to protect cells against peroxide was next evaluated. A dose-dependent protection of SH-SY-5Y cells was obtained by preincubation with either GSH or Ψ-GSH before exposure to peroxide (Figure 5). The activity of Ψ-GSH

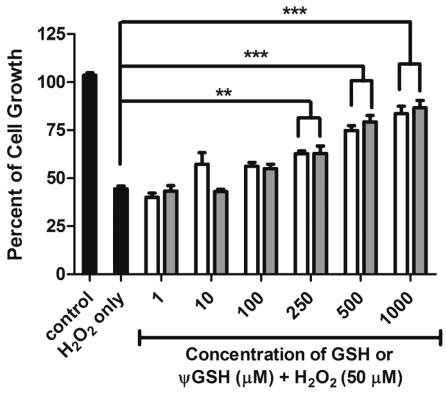

Figure 5. Reduction in the cytotoxicity of H_2O_2 in the presence of GSH and Ψ-GSH. Pretreatment of SH-SY-5Y cells with GSH or Ψ-GSH (1 mM) for 24 h prior to H_2O_2 (50 μM) exposure for 30 min showed a significant protection against peroxide toxicity. The protection observed due to GSH (white bars) and Ψ-GSH (gray bars) was comparable and dose-dependent with respect to their concentrations. The data are expressed as the (mean ± SEM) of three independent experiments (** $p < 0.001$; *** $p < 0.0001$).

was comparable to that of GSH. Intracellular ROS concentration in response to H_2O_2 (500 μM) exposure was found to be 2.8-fold over control cells ($p < 0.0001$). Co-incubation of H_2O_2 with GSH or Ψ-GSH (250 μM) led to reduction in ROS to the levels in control cells (Figure 6A). Similar results were obtained with ROS generated by MG treatment (1 mM, 180 min; Figure 6B), which was neutralized effectively by GSH or Ψ-GSH. These results demonstrate comparable antioxidant potency of Ψ-GSH to that of GSH.

Finally, we examined the ability of Ψ-GSH to traverse the blood brain barrier (BBB), which has active transport machinery for GSH. GSH uptake transporters are located on the luminal side and display broad substrate specificity.[31] The uptake of [^{3}H]-GSH by SH-SY-5Y cells at a concentration of 100 nM of [^{3}H]-GSH was determined in the presence of 1 μM, 100 nM and 10 nM of Ψ-GSH (Figure 7). GSH uptake was found to be inhibited in a dose-dependent manner by Ψ-GSH, the magnitude of which was comparable with that obtained in the presence of similar concentrations of cold GSH. This ascertains that the membrane transport mechanism for GSH is capable of recognizing Ψ-GSH. We have previously utilized Ψ-GSH as a carrier to transport BBB impermeable drugs into the brain.[21]

The studies in this report support our hypothesis of a metabolically stable GSH analogue being a viable GSH replacement. Ψ-GSH is recognized by the GSH transporter in the BBB. Ψ-GSH is successfully utilized by the cellular machinery that detoxifies MG, a major component of oxidative stress in Alzheimers' disease. In that regard, Ψ-GSH is a better substrate than all known alternative substrates for Glx-I, making it a valuable enzymological tool. It possesses the ability of GSH to counteract Aβ-induced intracellular ROS. As anticipated, Ψ-GSH is stable to γ-GT making its use as an antioxidant potentially more practical than GSH or glutamylcysteine. This stability to γ-GT enables it to protect cells against Aβ-induced toxicity for a significantly longer period when compared to GSH. Future studies will focus on evaluation of Ψ-GSH in animal models of Alzheimer's disease.

METHODS

Drugs and Reagents. Radiolabeled [^{3}H]-GSH was purchased from Perkin-Elmer Life Sciences (Waltham, MA). All other chemicals were purchased from Sigma (St. Louis, MO). Yeast glyoxalase I was purchased from Sigma. Aβ1-42 was purchased from American Peptide Company (Sunnyvale, CA). For all experiments, Aβ1-42 was dissolved in 100% 1,1,1,3,3,3-hexafluoro-2-propanol (HFIP) to a concentration of 1 mg/mL, sonicated in a water bath for 10 min, and dried under vacuum. The HFIP-treated Aβ1-42 was dissolved in dimethyl sulfoxide (DMSO) to a final concentration of 1 mM and stored at −20 °C. Asparthione and *S*-(*p*-bromobenzyl)-glutathione were synthesized in

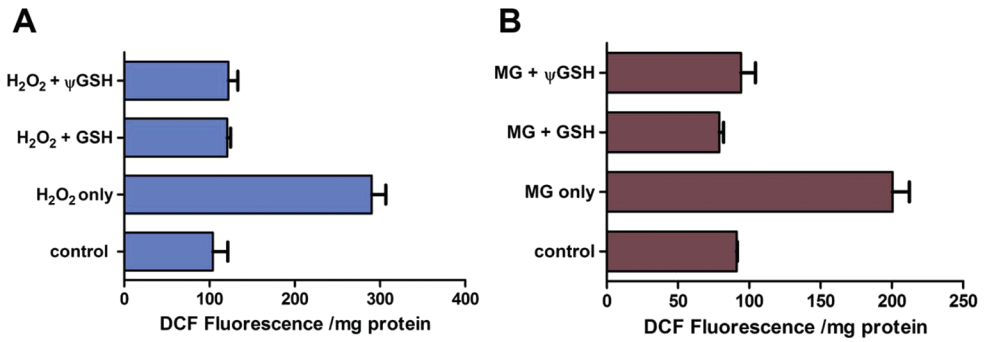

Figure 6. Measurement of ROS using DCFH-DA. Oxidative stress was induced in SH-SY-5Y cells by exposure to (A) H_2O_2 (500 μM) for 90 min or (B) MG (1 mM) for 180 min at 37 °C in the presence or absence of GSH or Ψ-GSH (250 μM). Increase in fluorescence of DCF was regarded as an indicator of oxidative stress as described in Methods. Both GSH and Ψ-GSH were efficient at reducing the ROS generated by peroxide and MG. The data are represented as the (mean ± SEM) of two independent experiments ($p < 0.0001$).

dx.doi.org/10.1021/cn200113z | *ACS Chem. Neurosci.* 2012, 3, 204–210

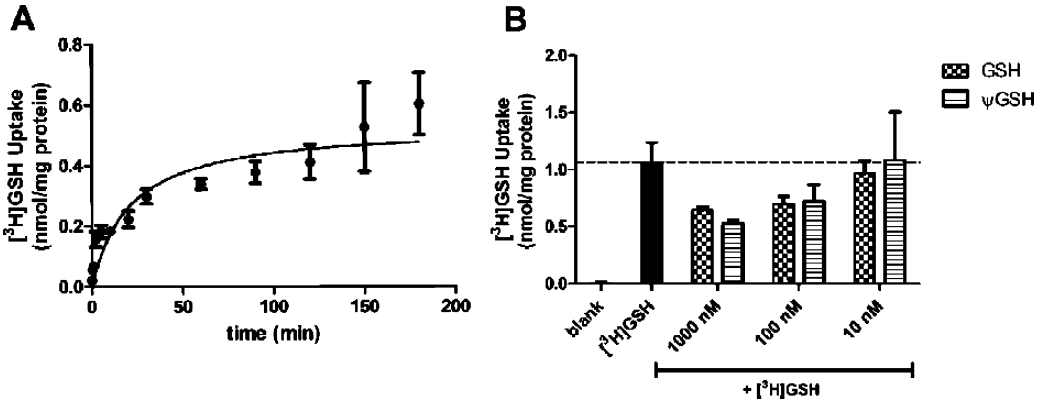

Figure 7. (A) Uptake kinetics of [^{3}H]GSH in SH-SY-5Y cells. SH-SY-5Y cells were exposed to [^{3}H]GSH (100 nM) at 37 °C for various time intervals and intracellular radioactivity was measured using scintillation counter. The net uptake was normalized to protein content in each well as described in Methods. The data are represented as the (mean ± SEM) of three independent experiments. (B) Inhibition of [^{3}H]GSH uptake by Ψ-GSH. Uptake of [^{3}H]GSH (1000 nM) in the presence and absence of GSH and Ψ-GSH (10, 100, and 1000 nM) was determined in SH-SY-5Y cells as described in Methods. The inhibition of [^{3}H]GSH uptake by Ψ-GSH was comparable to that by cold GSH. The data are represented as the (mean ± SEM) of three independent experiments ($p < 0.0001$).

our laboratory using a combination of previously published methods.[22,23] The cell culture media MEM, F12, and fetal bovine serum (FBS) were obtained from Invitrogen (Carlsbad, CA).

General Synthetic Procedures. All commercial chemicals were used as supplied unless otherwise indicated. Dry solvents (THF, Et_2O, CH_2Cl_2, and DMF) were dispensed under argon from an anhydrous solvent system with two columns packed with neutral alumina or molecular sieves. Flash chromatography was performed with Silica-P flash silica gel (silicycle, 230−400 mesh) with indicated mobile phase. All reactions were performed under inert atmosphere of ultrapure argon with oven-dried glassware. ^{1}H and ^{13}C NMR spectra were recorded on a Varian 300 MHz spectrometer. High resolution mass data were acquired on a Bruker Bio TOF-II spectrometer capable of positive and negative ion ESI source, using PPG or PEG as internal standards.

Synthesis of Ψ-GSH. To the tripeptide **1** (700 mg, 1.15 mmol) was added with stirring a mixture of CH_2Cl_2, TFA, and anisole in a ratio of 2:2:1. The flask was flushed with argon and stirring was continued at ambient temperature for 3 h. The progress of the reaction was monitored by LC-MS. Upon consumption of starting material, the reaction mixture was concentrated to dryness and the residue was triturated with ether. The white precipitate (Ψ-GSH-S−S*t*Bu) was filtered, washed with ether and utilized in the following step without further purification.

A solution of Ψ-GSH-S−S*t*Bu (0.40 g, 1.01 mmol) in 15 mL of *n*PrOH/H_2O (2:1) was adjusted to pH = 8.5 with 25% aq ammonia. *n*Bu_3P (400 μL, 1.51 mmol) was then added, and the reaction mixture was allowed to stir at ambient temperature for 2 h. The reaction mixture was then evaporated to dryness and the residue triturated with $CHCl_3$ (3 × 30 mL) to afford a clear oil. This oil was loaded on a column (15 g) of C-18 bound silica gel, and the column was eluted with water. Relevant fractions were evaporated to dryness to obtain an oil that was triturated with methanol to afford Ψ-GSH as a white solid (180 mg, 58%). Mp 165−167 °C; R_f = 0.50 (butanol/acetic acid/water; 4:1.5:2); $[\alpha]_D^{20}$ −16.1 (*c* 0.54, 1N HCl); ^{1}H NMR (300 MHz, D_2O) δ ppm 4.60 (q, *J* = 4.8, 8.4 Hz, 1H, α-CH:Cys), 4.48 (q, *J* = 4.8, 7.8 Hz, 1H, α-CH:Dap), 4.17 (m, 2H, CH_2:Gly), 3.68−3.62, 3.41−3.34 (2 m, 2H, β-CH_2:Dap), 3.24−2.98 (m, 2H, β-CH_2:Cys); ^{13}C NMR (75 MHz, CD_3OD-CF_3COOD) δ 174.5, 172.6, 170.5, 159.2 (C═O), 52.4 (α-C:Cys), 49.1 (α-C:Dap), 44.3 (β-C:Dap), 42.6 (CH_2:Gly), 31.5 (β-C:Cys); ESI-HRMS *m*/*z* 309.0798 $(M+H)^+$; $C_9H_{16}N_4O_6S + H^+$ requires 309.0869; reverse phase HPLC was run on Varian Microsorb column (C18, 5 μm, 4.6 × 250 mm) using two solvent systems with 0.5 mL/min flow rate and detected at 220 nm. Solvent system 1: 0.04 M TEAB (triethylammonium bicarbonate) in water/70% acetonitrile in water =1/1, t_R = 7.70 min, purity = 96.06%. Solvent system 2: 0.04 M TEAB in water/70% acetonitrile in water = 20 − 100% B linear, t_R = 13.67 min, purity =95.90%.

Cell Culture. The human neuroblastoma cell line, SH-SY-5Y, used in the present study was obtained from American Type Culture Collection (Manassas, VA). The cells were maintained in MEM:F12 (1:1) medium supplemented with 10% FBS, 100 units/mL penicillin and 100 units/mL streptomycin, and 1% NEAA (nonessential amino acid). Cells were grown at 37 °C in a humidified atmosphere with 5% CO_2/95% air.

Glyoxalase I Enzyme Kinetics Assay. The glutathione analogue, Ψ-GSH, and asparthione were examined for their ability to act substrates for the yeast glyoxalase I mediated reduction of MG. The commercial 40% methylglyoxal solution was distilled to remove polymerization products as described earlier (ref). Enzyme assays were performed (30 °C, 0.05 M phosphate buffer (pH 6.6)) using a thermostatted Beckman DU 7400 spectrophotometer. Fresh solutions of GSH, Ψ-GSH and asparthione were prepared on the day of the assays with distilled, deionized water. In each assay, the cell contained a total volume of 3.0 mL which was no more than 6.0 mM with respect to methylglyoxal and 1.3 mM with respect to GSH or its analogues. Sufficient amounts of glyoxalase I, in the presence of 0.1% bovine serum albumin as a stabilizing agent, were employed so as to afford an easily measurable initial rate that was followed by an increase in absorption at 240 nm. MG, GSH, or its analogues and buffer were added to a cuvette and allowed to stand for 6 min in the thermostatted compartment of the spectrophotometer to allow complete equilibration of the substrates with the hemimercaptal **2**. Hemimercaptal substrate concentrations were calculated from the concentrations of thiol peptide and methylglyoxal added, using a value of 3.1×10^{-3} M for the dissociation constant of the hemimercaptal at pH = 6.6. Data were analyzed utilizing an enzyme kinetics module of Sigmaplot 9.0 from Systat Software Inc.

γ-Glutamyltranspeptidase Assay. The stability of Ψ-GSH toward γ-GT mediated degradation was determined by incubating 100 μL of 10 mM solutions of GSH or Ψ-GSH (dissolved in 200 mM of 2-amino-2-methyl-1,3-propanediol buffer at pH 8.5) with 10 μL of 0.54 mg/100 μL of equine kidney γ-glutamyltranspeptidase in the above buffer in presence of 20 μL of acceptor dipeptide gly-gly (40 mM in the above buffer). After incubation for 1 h at 37 °C, compound from each tube was spotted on a silica gel TLC plate. The plates were developed alongside authentic predicted degradation products with the solvent system: 4:1.5:2; butanol/acetic acid/water. Visual detection of TLC spots was performed under UV and also by iodine and fluorescamine staining solution.

Inhibition of Glutathione Uptake by Ψ-GSH. The uptake experiment was performed under conditions described previously. Briefly, the cells were seeded in 24-well plates. After an overnight

incubation, the cells were treated with 100 nM concentration of [^{3}H]-GSH in uptake buffer (128 mM NaCl, 4.73 mM KCl, 1.25 mM $CaCl_2$, 1.25 mM $MgSO_4$, and 5 mM HEPES, pH = 7.4) in the presence or absence of Ψ-GSH at concentrations of 10, 100, and 1000 nM at 37 °C under 5% CO_2 for 30 min. At the end of incubation, the cellular uptake was terminated by washing three times with ice-cold PBS. Any remaining buffer was aspirated, and the cells were lysed with 1 mL of warm 0.1% SDS/0.1 N NaOH solution for a minimum of 45 min. Intracellular levels of radioactive GSH were determined using liquid scintillation counting. All resulting levels of GSH uptake were normalized to the total protein in each well using a BCA protein assay. All uptake experiments were performed in triplicate and statistically significant differences in uptake were evaluated using Graphpad Prism 5.1 (GraphpPad, La Jolla, CA) using a one-way ANOVA followed by a Dunnett's post hoc test with a false discovery rate of 0.05.

Cytotoxicity Studies. Protection against β-amyloid 1-42 cytotoxicity in SH-SY-5Y cells was measured by standard MTT assays. SH-SY-5Y cells were seeded in 96-well plates at the density of 30 000 cells/well. After overnight incubation, the cells were exposed to GSH or Ψ-GSH at a concentration of 1 mM for 24 h at 37 °C. After 24 h of incubation, the drug-containing medium was replaced with media containing 20 μM β-amyloid 1-42 peptide, and the incubation was allowed to continue for additional 24 h after the addition of the drugs. At the end of the incubation, 20 μL of MTT stock solution (5 mg/mL) was added to each well and incubated for 3 h at 37 °C. The MTT reaction medium was discarded and the purple-blue MTT formazan crystals were dissolved by the addition of 100 μL of 0.1 N HCl in isopropanol. The optical density (OD), a reflection mitochondrial function of the viable cells, was read directly with a microplate reader (BioTek SynergyHT, VT) at 580 nm and a reference wavelength of 680 nm. Concentration response graphs were generated for each drug using GraphPad Prism software (GraphPad Software, Inc., La Jolla, CA). Results are expressed as mean percent inhibition of β-amyloid toxicity with the standard error of the mean. In another set of experiments, cells were preincubated with a glyoxalase I inhibitor, *S*-(*p*-bromobenzylglutathione) (1 mM) for 24 h before addition of β-amyloid 1-42 peptide (20 μM).

Similar procedures were used for determining the protective effect of GSH and its analog against H_2O_2 cytotoxicity. After preincubation of cells with GSH or Ψ-GSH for 24 h, cells were exposed to H_2O_2 (50 μM) for 30 min and the media was replaced with fresh media. Cells were incubated for an additional 24 h after which the cell viability was the determined by the MTT assay as described earlier.

H_2O_2 and MG-Induced Cellular Oxidative Stress. SH-SY-5Y cells were cultured in 96-well black plates at the density of 10 000 cells/well and were allowed to reach confluence (~48 h). The cells were then treated with a solution of 2,7-dichlorofluorescin diacetate (DCFH-DA, 20 μM) in RPMI 1640 medium without FBS for 45 min. Extracellular DCFH-DA was removed by washing twice with PBS. To induce oxidative stress, the cells were treated with hydrogen peroxide (500 μM) or methylglyoxal (1 mM) in RPMI media without FBS in presence and absence of GSH or Ψ-GSH (250 μM) for 90 or 180 min at 37 °C in the dark. The cells were washed with PBS and then lysed by adding 250 μL of 90% DMSO/10% PBS for 10 min in the dark at room temperature with shaking. The fluorescence intensity in each well was measured in the fluorescence plate reader (BioTek SynergyHT, VT) at an excitation of 485 nm and an emission of 538 nm and normalized to the protein content in each well as determined by the BCA assay.[32]

Determination of Intracellular MG Concentration. SHSY5Y cells were seeded in a T150 flask and allowed to grow for 24 h. The next day, cells were treated with glucose (50 mM) in the presence and the absence of GSH or Ψ-GSH (500 μM). Cells without glucose treatment were used as a control. After 3 days of treatment, the cell pellet was collected and sonicated in 1 mL of PBS buffer to obtain cell lysates, which were derivatized as follows: 1 mL of cell lysate + 0.2 mL of 5 M $HClO_4$ + 0.2 mL of 10 mM 1,2 diaminobenzene + 0.1 mL of 1 μM 5-methylquinoxaline (internal std) + 0.5 mL of water to 2 mL of final volume. Samples were incubated at room temperature overnight and then centrifuged. The supernatant was passed through a C-18 SPE cartridge which had been prepared by flushing 2−4 mL of acetonitrile followed by 2−4 mL of 10 mM KH_2PO_4 (pH 2.4). After evaporation of the acetonitrile layer, the solid obtained was redissolved in 0.2 mL of 20% acetonitrile in 10 mM KH_2PO_4 (pH = 2.4). The concentration of MG derivative, 2-methylquinoxaline, was measured using a Beckman Coulter Gold chromatography system. The column was Varian Microsorb-MV 300-5 25 cm C18 column (4.6 mm internal diameter and 5 μm particle diameter). The mobile phase was 80 vol % of 10 mM KH_2PO_4 and 20 vol % of HPLC grade acetonitrile. The analysis conditions were as follows: detector wavelength, 315 nm; mobile phase flow rate, 1.0 mL/min; typical injection volume, 20 μL. Duplicate injections of each sample were made. Samples were calibrated by comparison with a 2-methylquinoxaline standard. The average retention time of 2-methylquinoxaline was 7.35 min.

Data Analysis. Data were analyzed statistically by unpaired or paired Student *t* tests, as appropriate. Statistical significance was set at $p < 0.05$.

■ ASSOCIATED CONTENT

Ⓢ Supporting Information

Thin layer chromatograms for the γ-GT assay, plots comparing protection of SH-SY-5Y cells from Aβ toxicity by GSH and Ψ-GSH at various time intervals. This material is available free of charge via the Internet at http://pubs.acs.org.

■ AUTHOR INFORMATION

Corresponding Author

*Mailing address: 8-123A Weaver Densford Hall, 308 Harvard St. SE, University of Minnesota, Minneapolis, Minnesota 55455. E-mail: vince001@umn.edu.

Author Contributions

S.S.M. performed experimental work, data analysis, and manuscript preparation. R.V. performed project inception, design, guidance, and manuscript preparation.

Funding

This research was supported by the funds from the Center for Drug Design at the University of Minnesota.

Notes

The authors declare no competing financial interest.

■ ACKNOWLEDGMENTS

We thank Jessica Williams for performing glyoxalase I enzyme kinetics assays.

■ REFERENCES

(1) Alzheimer's Association. (2010) *Alzheimer's disease facts and figures*. Retrieved, February 18, 2011, from http://www.alz.org/documents_custom/report_alzfactsfigures2010.pdf.

(2) Khachaturian, Z. S. (1985) Diagnosis of Alzheimer's disease. *Arch. Neurol. 42*, 1097−1105.

(3) Armstrong, R. A. (2011) The Pathogenesis of Alzheimer's Disease: A Reevaluation of the "Amyloid Cascade Hypothesis. *Int. J. Alzheimer's Dis. 2011*, 630865−630870.

(4) Markesbery, W. R. (1997) Oxidative stress hypothesis and Alzheimer's disease. *Free Radical Biol. Med. 23*, 134−147.

(5) Monnier, V. M., and Cerami, A. (1981) Nonenzymatic browning in vivo: possible process for aging of long lived proteins. *Science 30*, 491−493.

(6) Ma, H., Sylvain, L., Kotilinek, L., Steidl-Nochols, J. V., Sherman, M., Younkin, L., Younkin, S., Forster, C., Sergeant, N., Delacourte, A., Vassar, R., Citron, M., Kofuji, P., Boland, L. M., and Ashe, K. H. (2007) Involvement of β-site APP cleaving encyme 1 (BACE1) in amyloid precursor protein mediated enhancement of memory and

activity-dependent synaptic plasticity. *Proc. Natl. Acad. Sci. U.S.A. 104*, 8167−8172.
(7) Kamenetz, F., Tomita, T., Hsieh, H., Seabrook, G., Borchelt, D., Iwatsubo, T., Sisodia, S., and Malinow, R. (2003) APP processing and synaptic function. *Neuron 37*, 925−937.
(8) Teplow, D. B. (1998) Structural and kinetic features of amyloid beta-protein fibrillogenesis. *Amyloid 5*, 121−142.
(9) Vitek, M. P., Bhattacharya, K., Glendenig, J. M., Stopa, E., Vlassara, H., Bucala, R., Manogue, K., and Cerami, A. (1994) Advanced glycation end products contribute to amyloidosis in Alzheimer disease. *Proc. Natl. Acad. Sci. U.S.A. 91*, 4766−4770.
(10) Ko, S. Y., Lin, Y. P., Lin, Y. S., and Chang, S. S. (2010) Advanced glycation end products enhance amyloid precursor protein expression by inducing reactive oxygen species. *Free Radical Biol. Med. 49*, 474−480.
(11) Wiśniewski, H. M., Narang, H. K., and Terry, R. D. (1976) Neurofibrillary tangles of paired helical filaments. *J. Neurol. Sci. 27*, 173−181.
(12) Ledesma, M. D., Bonay, P., Colaço, C., and Avila, J. (1994) Analysis of microtubule-associated protein tau glycation in paired helical filaments. *J. Biol. Chem. 269*, 21614−21619.
(13) Alonso, A., Zaidi, T., Novak, M., Grundke-Iqbal, I., and Iqbal, K. (2001) Hyperphosphorylation induces self-assembly of tau into tangles of paired helical filaments/straight filaments. *Proc. Natl. Acad. Sci. U.S.A. 98*, 6923−6928.
(14) Busciglio, J., Lorenzo, A., Yeh, J., and Yankner, B. A. (1995) *β*-Amyloid fibrils induce tau phosphorylation and loss of microtubule binding. *Neuron 14*, 879−888.
(15) Liu, H., Wang, H., Shenvi, S., Hagen, T. M., and Liu, R. M. (2006) Glutatione metabolism during aging and in Alzheimer disease. *Ann. N.Y. Acad. Sci. 1019*, 346−349.
(16) Chen, C. N., Brown-Borg, H. M., Rakoczy, S. G., Ferrington, D. A., and Thompson, L. V. (2010) Aging impairs the expression of the catalytic subunit of glutamate cysteine ligase in soleus muscle under stress. *J. Gerontol., Ser. A 65*, 129−137.
(17) Adams, J. D. Jr., Klaidman, L. K., Odunze, I. N., Shen, H. C., and Miller, C. A. (1991) Alzheimer's and Parkinson's disease: brain levels of glutathione, glutathione disulfide and vitamin E. *Mol. Chem. Neuropathol. 14*, 213−226.
(18) Butterfield, D. A., and Kanski, J. (2001) Brain protein oxidation in age-related neurodegenerative disorders that are associated with aggregated proteins. *Mech. Ageing Dev. 122*, 945−962.
(19) Butterfield, A. D., Pocernich, C. B., and Drake, J. (2002) Elevated glutathione as a therapeutic strategy in Alzheimer's disease. *Drug Dev. Res. 56*, 428−437.
(20) Witschi, A., Reddy, S., Stofer, B., and Lauterburg, B. H. (1992) The systemic availability of oral glutathione. *Eur. J. Clin. Pharmacol. 43*, 667−669.
(21) More, S. S., and Vince, R. (2008) Design, synthesis and biological evaluation of glutathione peptidomimetics as components of anti-Parkinson prodrugs. *J. Med. Chem. 51*, 4581−4588.
(22) More, S. S., and Vince, R. (2009) Inhibition of glyoxalse-I: the first low-nanomolar tight-binding inhibitors. *J. Med. Chem. 52*, 4650−4656.
(23) Pileblad, E., and Magnusson, T. (1992) Increase in rat brain glutathione following intracerebroventricular administration of gamma-glutamylcysteine. *Biochem. Pharmacol. 44*, 895−903.
(24) Behrens, O. K. (1941) Coenzymes for glyoxalase. *J. Biol. Chem. 141*, 503−508.
(25) Queisser, M. A., Yao, D., Geisler, S., Hammes, H., Lochnit, G., Schleicher, E. D., Brownlee, M., and Preissner, K. T. (2009) Hyperglycemia impairs proteasome function by methylglyoxal. *Diabetes 59*, 670−678.
(26) Xu, J., Chen, S., Ahmed, S. H., Chen, H., Ku, G., Goldberg, M. P., and Hsu, C. Y. (2001) Amyloid-*β* peptides are cytotoxic to oligodendrocytes. *J. Neurosci. 21*, RC118−RC122.
(27) Vince, R., Daluge, S., and Wadd, W. B. (1971) Inhibition of glyoxalase-I by S-substituted glutathiones. *J. Med. Chem. 14*, 402−404.
(28) Hewitt, N., and Rauk, A. (2009) Mechanism of hydrogen peroxide production by copper-bound amyloid beta peptide: a theoretical study. *J. Phys. Chem. B 113*, 1202−1209.
(29) Behl, C., Davis, J. B., Lesley, R., and Schubert, D. (1994) Hydrogen peroxide mediates amyloid beta protein toxicity. *Cell 77*, 817−827.
(30) Milton, N. G. (2004) Role of hydrogen peroxide in the aetiology of Alzheimer's disease: implications for treatment. *Drugs Ageing 21*, 81−100.
(31) Kannan, R., Chakrabarti, R., Tang, D., Kim, K. J., and Kaplowitz, N. (2000) GSH transport in human cerebrovascular endothelial cells and human astrocytes: evidence for luminal localization of Na +-dependent GSH transport in HCEC. *Brain Res. 852*, 374−382.
(32) Wang, G., Gong, Y., Burczynski, F. J., and Hasinoff, B. B. (2008) Cell lysis with dimethyl sulphoxide produces stable homogenous solutions in the dichlorofluorescein oxidative stress assay. *Free Radical Res. 42*, 435−441.